reconstitute irradiated-disordered bone marrow, were successfully produced by transduction of the *hoxb4* [9] or *cdx4* [10] genes, suggesting that the transduction of exogenous genes might be a good strategy for the differentiation of specified cells from human iPS and ES cells.

Viral expression libraries have been constructed with gamma retrovirus-based vectors [11–13]. Although these libraries could theoretically introduce genes into mitotic cells, they can also potentially introduce genes in a way that frequently results in leukemia [14]. On the other hand, lentiviral vectors have excellent features for carrying transgenes, including high transduction efficiency leading to an ability to transduce dormant cells, constitutive and long-term expression of transgenes, and the capacity to transduce multiple genes at one time. Kawano et al. constructed a lentiviral library with amplified peripheral leukocyte cDNAs to identify molecules related to cellular resistance to HIV-1 entry and HIV-1-induced cell death [15]. However, a human fetal liver lentiviral cDNA library has not yet been developed.

In this study, we have successfully constructed a high-performance human fetal liver-derived lentiviral expression library, which contained a high number of individual clones, in order to develop a useful research tool for the field of hematopoiesis and/or hepatopoiesis, for future use in clinical regenerative medicine.

Materials and methods

Cells

Human 293T cells were maintained in Dulbecco's modified Eagle medium (DMEM) supplemented with 10% heat-inactivated fetal bovine serum (FBS), 100 U/ml penicillin, and 100 mg/ml streptomycin (Nacalai Tesque, Kyoto, Japan), in a humidified atmosphere containing 5% CO_2 at 37°C.

Construction of the lentiviral cDNA library

A CloneMiner cDNA library construction kit (Invitrogen, Carlsbad, CA) was used throughout for preparing the Lentiviral cDNA Library. Double-stranded cDNA was prepared from 5 μg of the human fetal liver poly $(A)^+$ RNA (Clontech, Palo Alto, CA), using Biotin-*att*B2-Oligo (dt) for priming. The blunted cDNA was then ligated to *att*B1 adapters and fractionated using cDNA size fractionation columns (Invitrogen). cDNA fractions (100 ng) >500 bp were incubated with pDONR222 (250 ng) and BP Clonase enzyme mix (Invitrogen) for 18 h at 25°C, and the resulting recombinant sample was electroporated into ElectroMAX DH10B competent cells (Invitrogen). The transformants were pooled, and the resultant entry cDNA library was prepared from pools of transformants using the JETSTAR2.0 plasmid purification kit (Genomed, Lohne, Germany). To generate the lentiviral cDNA vector library, the entry vector (300 ng) and the CSII-CMV-RfA vector (300 ng), which contained *att*R1 and *att*R2 sites, were incubated with LR Clonase enzyme mix (Invitrogen) for 18 h at 25°C. The resulting recombinant molecules were electroporated into ElectroMAX Stbl4 competent cells (Invitrogen), and then the transformants were pooled. To prepare the plasmids for the cDNA library, pools of transformants were plated on LB agar plates containing ampicillin (100 μg/ml), and plasmid purification was carried out from recovered transformants.

Determining the individual cDNA lengths in the constructed library

The entry cDNA library plasmids and the lentivirus vector cDNA library plasmids were digested with *Bsr*GI (New England Biolabs, Ipswich, MA), subjected to agarose gel electrophoresis, and visualized with ethidium bromide (Sigma, St. Louis, MO). The length of each cDNA was estimated from the sizes of the fluorescent of DNA bands.

Sequence analysis

cDNAs that were cloned into the CSII-CMV-RfA vector were sequenced with the forward (5′-CAAGCCTCAGACA GTGG-3′) and reverse (5′-AGCGTATCCACATAGCG-3′) primers using a BigDye Terminator v3.1 Cycle sequencing kit (Applied Biosystems, Foster City, CA) and an ABI PRISM 3100 Genetic Analyzer (Applied Biosystems). The sequences were compared with the DNA database from the DNA Data Bank of Japan using BLAST.

Lentivirus production and transduction with the lentiviral library

Briefly, 34 μg (1–2 × 10^5 cDNA clones) of the library was mixed with 40 μg of the packaging plasmids (pCAG-HIVg/p and pCMV-VSVG-RSV-Rev) in 3.5 ml of FBS-free DMEM medium, after which 370 μl of 1 mg/ml polyethylenimine (PEI) was added. After incubating for 15–30 min, the DNA/PEI complex was dropped onto semi-confluent 293T cells that were cultured in a T175 flask containing Opti-MEM medium for 3 h. These cells were then cultured in DMEM medium containing 10% FBS. Virus-containing medium was harvested 4 days after the transduction and concentrated by centrifugation (9,000 rpm, 6–8 h, 4°C). The resulting virus pellet was resuspended in 0.5–1 ml of complete DMEM and was used for overnight transduction of freshly prepared 293T cells.

Determining the individual cDNA lengths in the 293T cells infected lentiviral library

293T cells were transduced with the viral cDNA library and cloned using the limiting dilution method. Genomic DNA was isolated from each clone using the QIAamp DNA Micro Kit (Qiagen). The integrated cDNAs were amplified using PCR, with the forward primer (5′-TTCAGGTGTCGT GAACACGCTACCG-3′) and the reverse primer (5′-CCTC GATGTTAACTCTAGAGGATCC-3′). The Expand Long Template PCR System (Roche, Basel, Switzerland) was used for the PCR. The length of each cDNA was determined as described above.

Flow cytometry

Untransduced 293T cells and 293T cells that were transduced with the lentivirus library were resuspended at 1×10^6 cells/100 μl in PBS(−) supplemented with 2% FBS and incubated with FITC-conjugated anti-human glycophorin A (CD235a) antibody (BectonDickinson, Franklin Lakes, NJ). After 30 min at 4°C, the samples were washed twice with PBS/FBS solution and analyzed with a FACS Calibur. Cells were also stained with a FITC-conjugated isotype antibody as negative control. For cell sorting, immunomagnetic beads were used according to the manufacturer's instruction (Miltenyi Biotec, Gladbach, Germany).

Results

Construction of the entry cDNA library

To calculate the number of individual clones in the entry library, which was constructed with the gateway system from human fetal liver cDNA, 10^4, 10^5, and 10^6 dilutions of the entry cDNA library transformants (total three lots) were seeded onto LB-Amp plates and incubated overnight at 37°C. As shown in Table 1, the total entry library consisted of 7.87×10^8 individual clones calculated by counting the number of transformants. We randomly picked 103 colonies, prepared their plasmid DNAs, and digested them with *Bsr*GI. Each plasmid had an insert, and these inserts averaged 2.1 kb in size (Fig. 1a). The cDNA fragments ranged between 0.3 and 6.5 kb in this library, and >40% of the fragments (43.7%) were larger than 2 kb. In particular, about 7.8% of the large insert DNAs, those with fragments lager than 5 kb, were also confirmed. These results indicated that a high titer entry library had successfully been constructed.

Construction of the lentiviral cDNA library

The lentiviral cDNA library was also prepared using a recombination technique. As shown in Table 2, a library totaling 8.75×10^7 cfu was constructed. To estimate the average insert size in this library, we picked up 113 colonies and analyzed them as described above. These results showed the library had about a 2.1 kb average insert size (Fig. 1b). This library also contained cDNA fragments that were larger than 5 kb, and more than 40% of the fragments (41.6%) were larger then 2 kb. Sequence analysis of 48 clones demonstrated that >60% (25/40) had genes that encoded various full-length proteins including cytoplasmic enzymes, protein inhibitors, and membrane receptors (the other eight clones had unknown or genomic sequences; Table 3). Furthermore, the presence of typical liver and blood cell markers (such as albumin and hemoglobin) was also confirmed. These data indicated that a high-performance human fetal liver-derived lentiviral cDNA library had successfully been constructed.

Table 1 Summary of the transformants of the constructed entry cDNA library

Lot number	Dilution	Amount per plate (μl)	Colonies per plate	Titer (cfu/ml)	Average titer (cfu/ml)	Total volume (ml)	Total CFUs (cfu)
1	10^{-4}	100	210	2.1×10^7	2.37×10^7	12	2.84×10^8
	10^{-5}	100	20	2.0×10^7			
	10^{-6}	100	3	3.0×10^7			
2	10^{-4}	100	202	2.02×10^7	2.11×10^7	10	2.11×10^8
	10^{-5}	100	23	2.3×10^7			
	10^{-6}	100	2	2.0×10^7			
3	10^{-4}	100	218	2.18×10^7	2.43×10^7	12	2.92×10^8
	10^{-5}	100	21	2.1×10^7			
	10^{-6}	100	3	3.0×10^7			
							Final CFU count (cfu): 7.87×10^8

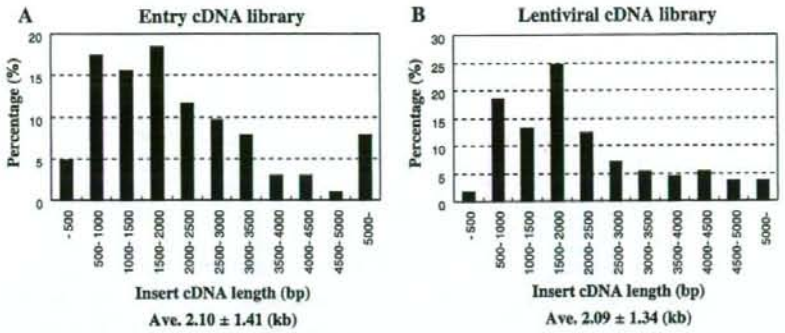

Fig. 1 The distribution of the cDNA fragments in the constructed entry (**a**) or lentiviral (**b**) cDNA libraries. More than 100 *E. coli* colonies in each library were randomly picked and their plasmid DNAs were prepared. Each plasmid was then digested with *Bsr*GI and analyzed. In each library, >40% of the cDNA fragments were >2 kb. Especially, large insert DNAs, namely, fragments >5 kb, were confirmed to be between 3.5% and 7.8% of the total. These data indicate that high titer entry and lentiviral libraries were successfully constructed

Table 2 Summary of the transformants of the lentiviral cDNA library

Lot number	Dilution	Amount per plate (μl)	Colonies per plate	Titer (cfu/ml)	Average titer (cfu/ml)	Total volume (ml)	Total CFUs (cfu)
1	10^{-3}	100	208	2.1×10^6	2.16×10^6	10	2.16×10^7
	10^{-4}	100	24	2.4×10^6			
	10^{-5}	100	2	2.0×10^6			
2	10^{-3}	100	397	3.97×10^6	3.96×10^6	10	3.96×10^7
	10^{-4}	100	49	4.9×10^6			
	10^{-5}	100	3	3.0×10^6			
3	10^{-3}	100	378	3.78×10^6	2.63×10^6	10	2.63×10^7
	10^{-4}	100	21	2.1×10^6			
	10^{-5}	100	2	2.0×10^6			
							Final CFU count (cfu): 8.75×10^7

Transduction of the lentivirus libraries into cultured cells

The lentiviral library was produced by transfecting $1–2 \times 10^5$ lentiviral cDNAs and an accessory plasmid DNA into freshly prepared 293T cells, after which single cell clones were isolated by limiting dilution. Genomic PCR analysis of 50 clones revealed that the transduction efficiency was 100% and most clones (49/50) had several transgenes (3–10). The average insert size of a transgene was about 1.1 kb and fragments >3 kb were not observed (Fig. 2). Next, to confirm the expression of the transgenes at the protein level, flow cytometric analysis was performed using anti-glycophorinA (GPA) antibody on 293T cells that were transduced with the viral library. GPA is major sialoglycoproteins of the human erythrocyte membrane. In early embryogenesis, hematopoietic, especially erythroid, development is observed in fetal liver, suggesting that various genes related to the development and differentiation of erythroid cells will be abundant in our library. The results showed that the frequency of GPA positive cells was slightly increased in the lentiviral library infected 293T cells compared with the non-transduced cells (0.4% vs. 0.04%, respectively; Fig. 3). This indicated that GPA derived from the library was expressed. To clarify this point more clearly, we sorted GPA positive cells with magnetic beads, cultured them for several days, and analyzed them by flow cytometry. The results showed that the frequency of GPA positive cells isolated from library transduced 293T cells was dramatically increased (up 65.4%), compared to that from the non-transduced cells. These results demonstrated that our lentiviral library could transduce exogenous genes into target cells and furthermore that these genes were expressed in these cells at the protein level.

Table 3 Sequence analysis of the lentiviral cDNA library

No.	Inserted length (kb)	Gene	Genbank accession No.	cds size (bp)	Status
1	2	Angiotensinogen (AGT)	NM_000029	1,458	F
2	2.2	Interleukin 10 receptor, beta (IL10RB)	NM_000628	978	F
3	1.8	EEF1A1	NM_001402	1,389	P
4	3.3	Albumin	BC039235	1,884	F
5	3.5	Poliovirus receptor (PVR)	BC015542	1,254	F
6	3.6	SH3-domain GRB2-like endophilin B2 (SH3GLB2)	BC014635	1,188	F
7	2.55	Stearoyl-CoA desaturase (SCD)	AF097514	1,080	P
8	0.9	Ribosomal protein S3A	BC001708	795	F
9	1.6	Heterogeneous nuclear ribonucleoprotein A1 (hnRPA1)	BC071945	963	F
10	1.5	Fibrinogen beta chain	BC107766	1,476	P
11	1.3	Protein inhibitor of activated STAT3 (PIAS3)	AB021868	1,860	P
12	0.7	Hemoglobin, alpha 2 (HBA2)	BC008572	429	F
13	1.4	Aldo-keto reductase family 1, member C1 (AKR1C1)	BC020216	972	F
14	2.7	Damage-specific DNA binding protein 1 (DDB1)	BC011686	3,423	P
15	1.3	Unknown	AC016525		
16	1.3	Glyceraldehyde-3-phosphate dehydrogenase (GAPDH)	BC029618	1,008	F
17	1.7	Unknown	AK128092		
18	0.9	Ferritin, light polypeptide (FTL)	BC004245	528	F
19	1.7	Insulin-like growth factor II (IGF-2)	X07868		P
20	0.8	Heat shock 60 kDa protein 1 (chaperonin)	BC073746	1,722	P
21	4.5	TP53 apoptosis effector variant, PERP	BC010163	582	F
22	0.65	Putative MAPK activating protein	AB097053	1,224	P
23	1.4	Non-specific DNA			
24	1.9	Aspatate aminotransferase 1	BC000498	1,242	F
25	7.3	Aconitase1, soluble (ACO1)	BC018103	2,670	F
26	2.8	Solute carrier family 25, member 46	BC017169	1,257	F
27	1.7	Ribonuclease P 14 kDa subunit	BC012017	375	F
28	1	Testis enhanced gene transcript (BAX inhibitor 1)	BC000916	714	P
29	1.5	Serpin peptidase inhibitor, clade A, member 1	BC015642	1,257	F
30	3.9	Histidine acid phosphatase domain containing 1	BC024591		P
31	0.65	Hemoglobin, alpha 2 (HBA2)	BC008572	429	F
32	5.7	Unknown	AF214636		
33	1.1	Haptoglobin	BC121125	1,221	P
34	1.5	Cross-immune reaction antigen (VCIA1)	AY858798	1,314	F
35	2.2	Albumin	BC039235	1,884	F
36	1.3	Unknown	AL365360		
37	0.3	ATPase, Na^+/K^+ transporting, beta 3 polypeptide	BC011835	840	P
38	2	Decorin (DCN)	BC005322	1,080	F
39	0.65	Ribosomal protein L32 pseudogene 3	BC053996		P
40	0.6	Wilm's tumor-related protein (QM)	M64241	645	F
41	0.7	Hemoglobin, beta	BC007075	444	F
42	1.3	Serpin peptidase inhibitor, clade A, member 3	BC070265	288	F
43	1.4	ras homolog gene family, member B	BC066954	591	P
44	1.7	Genomic DNA	AY495330		
45	1.7	Genomic DNA	DQ862537		
46	3.9	Genomic DNA	AL024498		
47	3	Genomic DNA	AL035461		
48	0.6	Hemoglobin, alpha 2 (HBA2)	BC008572	429	F

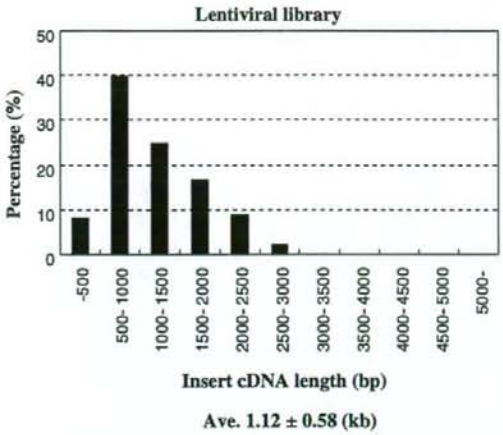

Fig. 2 The distribution of transgene length in the lentiviral library infected cells. After 293T cells were transfected with 1–2 × 10^5 lentiviral cDNAs and accessory plasmids, a lentiviral library was produced. Freshly prepared 293T cells were transduced with this virus library, and single cell clones were isolated by limiting dilution. Genomic PCR analysis of 50 clones revealed that the average transgene insert size was ~1.1 kb, and fragments >3 kb were not observed

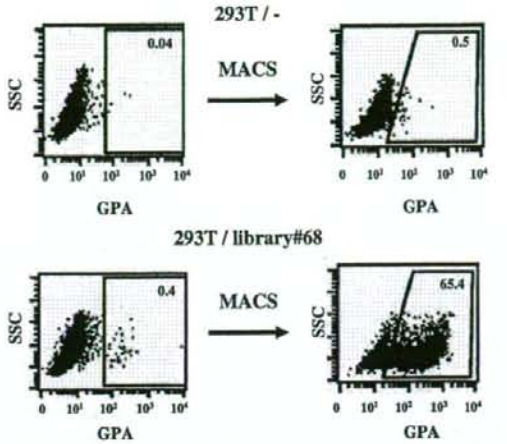

Fig. 3 Transgenic expression of the lentiviral library by flow cytometry. To confirm the expression of the transgenes at the protein level, virally transduced 293T cells were analyzed using flow cytometry with anti-glycophorinA (GPA). GPA positive cells were slightly increased in the lentiviral library transduced 293T cells (0.4%) compared with the non-transduced cells (0.04%). These GPA positive cells were sorted using magnetic beads, cultured for several days, and analyzed by flow cytometry. These results showed that GPA positive cells, which were isolated from the lentiviral library transduced 293T cells, were dramatically increased (65.4%) compared to non-transduced cells

Discussion

The library that we constructed in this study had 8.75 × 10^7 individual clones (100% of which had inserted DNA). The average insert length was about 2.1 kb. Sequence analysis demonstrated that more than 60% of these genes encoded full-length proteins. Moreover, high transduction efficiency was confirmed in cultured cells, and a transduced gene was translated and localized correctly. Kawano et al. successfully constructed a peripheral leukocyte-derived lentiviral cDNA library, which contained 8 × 10^7 primary clones and an average insert size of 1.26 kb [15]. Our library had almost the same number of insert cDNAs and a larger insert size. Notably, the average size of a gene that was transduced by our virus library was also longer (1.12 vs. 0.71 kb). These results demonstrate that a high-performance human fetal liver-derived lentiviral library was successfully constructed.

Lentiviral vectors can efficiently transduce both dividing and non-dividing cells, including blood and stem cells, which can generally be transduced with a low transduction efficiency [16]. In our experiment, most of the clonal virus-library transduced 293T cells had multiple (>3) transductions, suggesting that the transduction efficiency was high.

In early embryogenesis, most hepatopoietic and hematopoietic development (especially erythroid) is observed in fetal liver, suggesting that various genes related to the development and differentiation of the liver and blood will be abundant in our library. In line with this, some typical hepatocytic and erythroid cell markers (such as albumin and hemoglobin) were identified in our library. Thus, this fetal liver lentivirus library may be a powerful tool for the functional screening and targeting of novel genes that specify hepatocytic and hematopoietic cell development and differentiation.

A method for deriving iPS cells has been recently established [5–7], and therefore, organ regeneration will be a popular treatment for repairing damaged organs. The bone marrow and liver may be good candidates for target organs that require regeneration. Our fetal liver cDNA library may be a very useful tool for determining the genes that are important for differentiating iPS cells into hematopoietic cells or hepatopoietic cells. For example, one could screen ES cells and/or cytokine-dependent cell lines to find novel hematopoietic genes. We previously reported a highly efficient method for differentiating hematopoietic cell from primate ES cells by transducing the *tal1/scl* gene [8]. By combining this system with our fetal liver library, we may be able to direct the production of hematopoietic stem cells from ES cells, which may allow us to substantially impact the field of reproductive medicine in the near future.

References

1. Wong BY, Chen H, Chung SW et al (1994) High-efficiency identification of genes by functional analysis from a retroviral cDNA expression library. J Virol 68:5523–5531
2. Kassner PD (2008) Discovery of novel targets with high throughput RNA interference screening. Comb Chem High Throughput Screen 11:175–188. doi:10.2174/138620708783877744
3. Caldwell JS (2007) Cancer cell-based genomic and small molecule screens. Adv Cancer Res 96:145–173. doi:10.1016/S0065-230X(06)96006-0
4. Jones AK, Buckingham SD, Sattelle DB (2005) Chemistry-to-gene screens in *Caenorhabditis elegans*. Nat Rev Drug Discov 4:321–330. doi:10.1038/nrd1692
5. Takahashi K, Tanabe K, Ohnuki M et al (2007) Induction of pluripotent stem cells from adult human fibroblasts by defined factors. Cell 131:861–872. doi:10.1016/j.cell.2007.11.019
6. Nakagawa M, Koyanagi M, Tanabe K et al (2008) Generation of induced pluripotent stem cells without Myc from mouse and human fibroblasts. Nat Biotechnol 26:101–106. doi:10.1038/nbt1374
7. Yu J, Vodyanik MA, Smuga-Otto K et al (2007) Induced pluripotent stem cell lines derived from human somatic cells. Science 318:1917–1920. doi:10.1126/science.1151526
8. Kurita R, Sasaki E, Yokoo T et al (2006) Tal1/Scl gene transduction using a lentiviral vector stimulates highly efficient hematopoietic cell differentiation from common marmoset (*Callithrix jacchus*) embryonic stem cells. Stem Cells 24:2014–2022. doi:10.1634/stemcells.2005-0499
9. Kyba M, Perlingeiro RC, Daley GQ (2002) HoxB4 confers definitive lymphoid-myeloid engraftment potential on embryonic stem cell and yolk sac hematopoietic progenitors. Cell 109:29–37. doi:10.1016/S0092-8674(02)00680-3
10. Wang Y, Yates F, Naveiras O et al (2005) Embryonic stem cell-derived hematopoietic stem cells. Proc Natl Acad Sci USA 102:19081–19086. doi:10.1073/pnas.0506127102
11. Rayner JR, Gonda TJ (1994) A simple and efficient procedure for generating stable expression libraries by cDNA cloning in a retroviral vector. Mol Cell Biol 14:880–887
12. Whitehead I, Kirk H, Kay R (1995) Expression cloning of oncogenes by retroviral transfer of cDNA libraries. Mol Cell Biol 15:704–710
13. Kitamura T (1998) New experimental approaches in retrovirus-mediated expression screening. Int J Hematol 67:351–359. doi:10.1016/S0925-5710(98)00025-5
14. Hacein-Bey-Abina S, Von Kalle C, Schmidt M et al (2003) LMO2-associated clonal T cell proliferation in two patients after gene therapy for SCID-X1. Science 302:415–419. doi:10.1126/science.1088547
15. Kawano Y, Yoshida T, Hieda K et al (2004) A lentiviral cDNA library employing lambda recombination used to clone an inhibitor of human immunodeficiency virus type 1-induced cell death. J Virol 78:11352–11359. doi:10.1128/JVI.78.20.11352-11359.2004
16. Bai Y, Soda Y, Izawa K et al (2003) Effective transduction and stable transgene expression in human blood cells by a third-generation lentiviral vector. Gene Ther 10:1446–1457. doi:10.1038/sj.gt.3302026

Available online at www.sciencedirect.com
ScienceDirect
Biomedicine & Pharmacotherapy xx (2008) 1–12
BIOMEDICINE & PHARMACOTHERAPY
www.elsevier.com/locate/biopha

Original article

Tumor growth suppression by adenovirus-mediated introduction of a cell growth suppressing gene *tob* in a pancreatic cancer model

Hironobu Yanagie [a,b,*], Tuyoshi Tanabe [c], Hidetoshi Sumimoto [d], Hirotaka Sugiyama [b], Satoru Matsuda [e], Yasumasa Nonaka [f], Naoko Ogiwara [g], Katsunori Sasaki [g], Kensaburo Tani [h], Shinichi Takamoto [b,i], Hiroyuki Takahashi [a,b], Masazumi Eriguchi [b,j]

[a] *Department of Cardiac Surgery, Cooperative Unit of Medicine and Engineering Research, The University of Tokyo Hospital, Tokyo 113-8655, Japan*
[b] *Department of Nuclear Engineering and Management, Graduate School of Engineering, The University of Tokyo, Tokyo 113-8655, Japan*
[c] *National Institute of Advanced Industrial Science and Technology, Ibaragi 305-8562, Japan*
[d] *Division of Cellular Signaling, Institute for Advanced Medical Research, Keio University School of Medicine, Tokyo 160-8582, Japan*
[e] *Department of Molecular Pathogenesis, Nagoya University School of Medicine, Aichi 466-8560, Japan*
[f] *Department of Surgery, Hoyo Hospital, Iwate 028-3111, Japan*
[g] *Department of Anatomy, Shinshu University School of Medicine, Nagano 390-8621, Japan*
[h] *Medical Institute of Bioregulation, Kyusyu University, Fukuoka 874-0838, Japan*
[i] *Department of Cardiac Surgery, The University of Tokyo Hospital, Tokyo 113-8655, Japan*
[j] *Department of Microbiology, Syowa University School of Pharmaceutical Sciences, Tokyo 142-8555, Japan*

Received 18 April 2008; accepted 29 April 2008

Abstract

TOB (transducer of ErbB-2) is a tumor suppressor that interacts with protein-tyrosine kinase receptors, including ErbB-2. Introduction of the *tob* gene into NIH3T3 cells results in cell growth suppression. In this study, we evaluated the effect of *tob* expression in pancreatic cell lines (AsPC-1, BxPC-3, SOJ) and discuss the tumor-suppressing effects of adenoviral vector expressing *tob* cDNA. We first measured the levels of endogenous *tob* mRNA being expressed in all pancreatic cancer cell lines. Then, we examined the effect of adenoviral vector containing *tob* cDNA (Ad-*tob* vector) on cancer cell lines. The viral vector was expanded with transfection in 293 cells. The titer of the vector was 350×10^6 pfu/ml. These cancer cells were able to be transfected with MOI 20 without adenoviral toxicity. The transfection of Ad-*tob* vector results in growth suppression of SOJ and AsPC-1 cell lines. The magnitude of the expression of the Ad-*tob* gene in cancer is correlated to tumor suppressive activity. We prepared pancreatic cancer peritonitis models using a peritoneal injection of AsPC-1 cells. In this model, bloody ascites and multiple tumor nodules were seen at the mesentery after 16 days. AdCA*tob* (50×10^6 pfu/day) was administered from day 5 to day 9 after 4 days of peritoneal injection of 2×10^6 AsPC-1 cells. Tumor growth suppression occurred 10 days after peritoneal injection of AdCA*tob* compared with the control group. There were no tumor nodules in the abdomen and no bloody ascites. These results suggest that the peritoneal injection of AdCA*tob* has potential to suppress the formation of pancreatic cancer peritonitis, and can be applied for chemotherapy-resistant cancer peritonitis.
© 2008 Elsevier Masson SAS. All rights reserved.

Keywords: *Tob* gene; Tumor suppressor gene; Adenovirus vector; Gene therapy

1. Introduction

Pancreatic cancer is one of the leading causes of cancer deaths in the world. Diagnosis of pancreatic cancer is difficult,

* Corresponding author. Department of Cardiac Surgery, The University of Tokyo Hospital, 7-3-1 Hongo, Bunkyo-ku, Tokyo 113-8655, Japan. Tel.: +81 3 5800 9194; fax: +81 3 5800 9195.
E-mail addresses: yanagie@n.t.u-tokyo.ac.jp, h.yanagie@gmail.com (H. Yanagie).

0753-3322/$ - see front matter © 2008 Elsevier Masson SAS. All rights reserved.
doi:10.1016/j.biopha.2008.04.010

Please cite this article in press as: Yanagie H et al., Tumor growth suppression by adenovirus-mediated introduction of a cell growth suppressing gene *tob* in a pancreatic cancer model, Biomed Pharmacother (2008), doi:10.1016/j.biopha.2008.04.010

and once metastasis to the liver or peritoneal dissemination has occurred, current treatments, including surgery and chemotherapy, are difficult to induce complete remission [1].

Advances in science and technology for direct gene transfer into living animals have provided opportunities to develop treatment modalities of malignancies by somatic gene therapy [2–5].

TOB (transducer of ErbB-2) is a 45 kDa tumor suppressor that interacts with protein-tyrosine kinase receptors, including ErbB-2 [6,7]. ErbB-2 phosphorylates and interacts with Shc, which participates between active tyrosine protein kinases to the Ras signaling pathway. A point mutation or an elevated expression of ErbB-2 is commonly observed in pancreatic cancers and breast cancers. Matsuda et al. reported that the carboxy-terminal half of TOB is relevant to its interaction with ErbB-2 and the amino-terminal half is homologous to the growth suppressor protein BTG-1, and introduction of the *tob* gene into NIH3T3 cells results in cell growth suppression [6,8–10]. Expression of BTG-1 is high in quiescent cells and decreases when cells enter the growth cycle, suggesting that the gene product is inhibitory to G0/G1 progression. The *tob* is localized on chromosome 17q21, telomeric to the BRCA 1 locus.

Using the anti-proliferative function of TOB, here we evaluated *tob* expression in pancreatic cancer cell lines and discussed its potential as a useful candidate for genetic therapy of pancreatic cancer peritonitis with peritoneal (ip) injection of recombinant adenovirus vector containing the *tob* gene (AdCA*tob*) *in vitro* and *in vivo*.

2. Materials and methods

2.1. Target tumor cells, mice and antibodies

The human pancreatic carcinoma cell line SOJ and AsPC-1 producing carcinoembryonic antigen (CEA), were maintained in RPMI1640 medium (Hazleton Biologics, Inc., Kansas, USA) supplemented with 10% fetal calf serum (Cell Culture Laboratories, Ohio, USA) and 100 $\mu g\,ml^{-1}$ kanamycin. All cultures were incubated in high moisture air with 5% CO_2 at 37 °C. The medium was changed three times a week.

Male BALB/*cnu/nu* mice were obtained from Nihon SLC (Shizuoka, Japan) and used at 6–7 weeks of age. In each experiment, mice of similar age and weight were selected. Mice were housed in plastic cages and maintained in an air-conditioned room. The procedures for tumor implantation and sacrifice of the animals were in accordance with approved guidelines of the Institution's Animal Ethics Committee.

Mouse anti-human TOB monoclonal antibody (IgG 2a), 4B1, was obtained from Immuno-Biological Laboratories (Gunma, Japan).

2.2. Construction of plasmid

Expression plasmid pMIK-*tob* was constructed by inserting the 1.3 kbp *tob* cDNA fragment into pMIK vector (a derivative of pME18S, kindly provided by Dr. K. Maruyama, DNAX Res. Inst., CA, USA) [6].

2.3. Northern blot analysis

Total RNA of cancer cells was extracted by the guanidium isothiocyanate method. RNA samples (10 μg) were separated and blotted following the general protocol. One kbp *Hin*d III fragment of λ *tob* cDNA was used as a probe labeled with α-^{32}P-dCTP [6].

2.4. Recombinant adenovirus preparation

Adenovirus vector containing the *tob* driven by CAG promoter (AdCA*tob*) was prepared in this study following the method described previously [11–13]. Briefly, the 1.2 kb human *tob* fragment was blunt ended and subcloned into downstream of the CAG promoter of adenovirus vector. This expression cassette was subcloned into the *Swa*I site of the pAdex1cw cosmid, resulting in pAdex1*tob*. The pAdex1cw is a 42 kb cosmid containing a 31 kb adenovirus type 5 genome lacking *E1A*, *E1B*, and *E3* genes, as described previously. The expression cosmid cassette and adenovirus DNA-terminal protein complex were cotransfected into 293 cells by calcium phosphate precipitation. The recombinant viruses were propagated with 293 cells and viral solution was stored at −80 °C. The titers of viral stocks were determined by plaque assay on 293 cells. Adenovirus containing the *lacZ* gene coding for the bacterial enzyme β-galactosidase (AdCA*lacZ*) was used as a control to measure the efficiency of tumor cell infection.

2.5. Adenovirus-mediated lac Z expression in vitro

The pancreatic cancer cell lines were plated at a density of 50×10^3 cell/well in 24-well culture plates (Iwaki Glass, Tokyo, Japan) 12 h before AdCA*lacZ* infection. Then, culture medium was replaced with medium containing varying amounts of adenovirus per cell (MOI). After 48 h, the cells were stained with X-gal (Wako Ltd., Tokyo, Japan) and the number of β-galactosidase-positive cells was counted in order to demonstrate the transfection efficiency [13].

2.6. Cell growth assay

Human pancreatic cancer cell lines (50×10^3 cell) were cultured in 60 mm tissue culture dishes (Corning Glass Works, NY, U.S.A.) for 12 h. Then, the culture medium was replaced with suspensions of AdCA*lacZ* or AdCA*tob* at an MOI of 20. After transfection, the medium was changed every other day. Cell growth was assessed by counting the number of live cells on the indicated day after transfection. The results are the means ± SD from three independent experiments.

2.7. Protein immunoblotting

Six days after transfection of AdCA*lacZ* or AdCA*tob* into the pancreatic cancer cell lines, total protein was isolated by

Please cite this article in press as: Yanagie H et al., Tumor growth suppression by adenovirus-mediated introduction of a cell growth suppressing gene *tob* in a pancreatic cancer model, Biomed Pharmacother (2008), doi:10.1016/j.biopha.2008.04.010

lysis in 0.5 ml 1% NP-40 (Sigma). The lysates (100 μg protein) were electrophoresed on a 10% SDS-PAGE and transferred to nitrocellulose (Nytran, Schleicher & Schuell, Keene, NH) [14]. Western analysis was performed with the anti-TOB monoclonal antibody using a second antibody conjugated to peroxidase. The preparations were visualized with diaminobenzidine.

2.8. In vivo tumor experiments

2.8.1. Establishment of tumors in nude mice

We prepared pancreatic cancer peritonitis models using intraperitoneal (ip) injection of AsPC-1 pancreatic cancer cells. AsPC-1 cells were trypsinized, washed once with RPMI1640 and suspended in RPMI1640 at 1, 2, 5 or 10×10^6 cells/0.2 ml; a 0.2 ml cell suspension was injected into each nude mouse peritoneally.

2.8.2. Inhibition of tumor growth in vivo

In order to examine the tumor suppressor effect of the *tob* on the formation of pancreatic cancer peritonitis, ip injections of AdCA*tob* or AdCA*lac*Z were performed in tumor-bearing mice of a cancer peritonitis model. Peritoneal injection of AdCA*tob* or AdCA*lac*Z (50×10^6 pfu/0.2 ml/day, from day 5 to day 9) after 4 days of ip injection of AsPC-1 cells (2×10^6, doubling time 2–3 days). After 16 days of tumor inoculation, the mice were sacrificed and tumor formations investigated in the abdominal cavity.

2.8.3. Pathological evaluation of tumors in nude mice

At 16 days of follow-up, tumors from AdCA*tob*-, AdCA*lacZ*-treated groups and the non-treated control group were evaluated for differences between the control and the experimental groups by analyzing the anti-TOB immunostained sections of each tumor. Formalin-fixed paraffin-embedded *in vivo* experimental tissues were cut at 4–5 μm, dried at 60 °C, deparaffinized, and hydrated with distilled water. Endogenous peroxidase activity was blocked with 3% hydrogen peroxidase in PBS, followed by rinsing in several changes of distilled water and PBS. Immunochemical studies were performed using the avidin–biotin–peroxidase complex method of Hsu et al. in the following manner: sections were blocked with normal rabbit serum for 30 min at room temperature and incubated with mouse anti-human TOB monoclonal antibody (clone 4B1, 1:100 dilution) for 30 min at room temperature. HISTOFINE SAB-PO (M) kit (Nichirei Co. Ltd., Tokyo, Japan) was used to apply biotinylated anti-mouse IgG/IgA/IgM and avidin–biotin–peroxidase complexes, incubating for 10 min at room temperature. The immunoperoxidase staining reaction was visualized by using 0.5% dimethyl-aminoazobenzene in 0.61 M Tris buffer (pH 7.4) containing 0.03% hydrogen peroxidase.

3. Results

3.1. Northern blot analysis of endogenous tob transcripts in pancreatic cancer cell lines

The endogenous *tob* mRNA was expressed in the three pancreatic cancer cell lines (Fig. 1). The level of *tob* mRNA of SOJ cells was low, but that of AsPC-1 cells was high (A). The overexpression of *c-erbB-2* mRNA was shown in BxPC-3 and AsPC-1 cells (B).

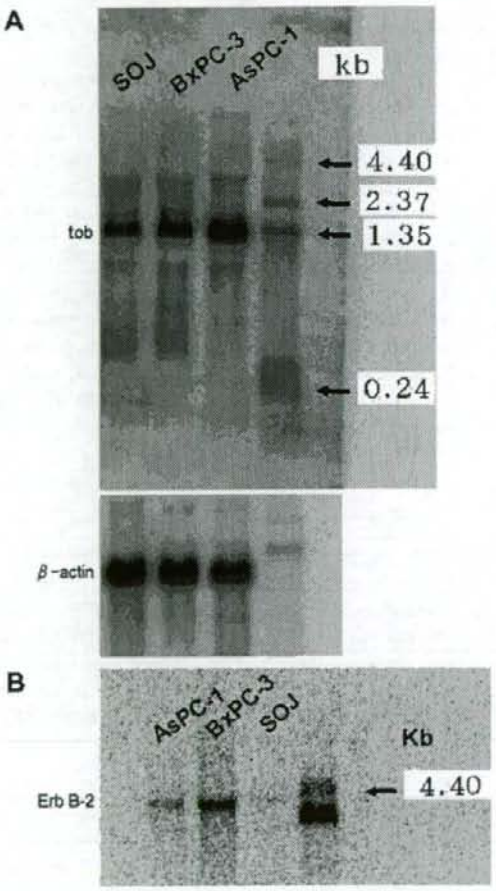

Fig. 1. Expressions of *tob*, *β-actin* (A) and *erbB-2* (B) mRNA in pancreatic cancer cell lines. Three human pancreatic cancer cell lines, AsPC-1, BxPC-3, and SOJ, were used in this experiment. (A) *tob* mRNAs are shown as a 1.3 kb band in the left side (upper panel of A). Total RNA was extracted and processed for Northern blot analysis as described in Section 2. A 10 μg of RNA were loaded in each lane. Standard molecular weights are shown on the right side as arrows. Internal control of the expression level of mRNA is shown as *β-actin* mRNA. (B) Expression level of *erbB-2* mRNAs is also compared among pancreatic cancer cell lines. Four kb bands corresponding to *erbB-2* mRNA are indicated by an arrow.

Please cite this article in press as: Yanagie H et al., Tumor growth suppression by adenovirus-mediated introduction of a cell growth suppressing gene *tob* in a pancreatic cancer model, Biomed Pharmacother (2008), doi:10.1016/j.biopha.2008.04.010

3.2. Adenovirus-directed lacZ gene transfer in pancreatic cancer cell lines in vitro

Use of a recombinant β-gal adenovirus AdCA*lacZ* allowed us to establish the measures of gene transfer efficiency in pancreatic cancer cells. Three human pancreatic cancer cell lines, AsPC-1, BxPC-3, and SOJ were used as target cells for the vector. These cell lines were transfected with AdCA*lacZ* at different MOIs (Fig. 2). The *lacZ* was expressed in all cell lines, in parallel with the increase in MOI. There was no significant difference in transfection efficacy among the cell lines, indicating that cell lines are susceptible to adenovirus transfection.

3.3. Tumor suppression by transfection of AdCAtob

In order to examine the tumor suppressor effect of the *tob* gene on the growth of cancer cells, the cells were transfected with AdCA*lacZ* or AdCA*tob* at an MOI of 20. The cells could be transfected with MOI 20 without adenoviral virulence. SOJ and AsPC-1 cell lines transfected with AdCA*tob* vector showed growth suppression (Fig. 3A). SOJ and AsPC-1 cells expressed exogenous *tob* mRNA, and were enlarged and megakaryocytic with many granules in the cytoplasm (Fig. 3B). The characteristics resembled those of senescent cells. Anti-proliferative activity of TOB seems to be well correlated with the level of its expression. In comparison with AdCA*lacZ*, the two-fold growth suppression was shown in the SOJ cell line expressing a good amount of TOB (Figs. 3A and 4).

3.4. Exogenous tob expression

TOB expression was analyzed with Western blot analysis of lysates of pancreatic cancer cell lines after transfection of AdCA*lacZ* or AdCA*tob*. As shown in Fig. 4, an exogenous 45 kDa band was detected in all transfected cell lines. Tob was successfully introduced, especially into SOJ cells, and the magnitude of the expression of TOB is correlated to tumor growth suppressive activity, as shown in Fig. 3A.

3.5. Pathological findings of tumors treated with AdCAtob vector: adenovirus-mediated tob expression in vitro

Expression of exogenous TOB (45 kDa) was confirmed by immuno-cytostaining of cells. AsPC-1 cells were plated at a density of 50×10^3 cells/well in a 24-well culture plate 12 h before AdCA*tob* infection. Then, cells were transfected with AdCA*tob* vector (MOI 20). After 72 h, cells were spinned down and stained with anti-TOB monoclonal antibody 4B1 in order to determine the expression of TOB. AsPC-1 cells showed the expression of TOB with AdCA*tob* transfection (Fig. 5).

3.6. Electronmicroscopic findings

We noted a dramatic change in the light scatter pattern of AsPC-1 cells upon induction of *tob* expression. Using transmission electron microscopy, we found that TOB-overexpressing AsPC-1 cells showed degradation of the nucleus and many autophagosomes and electron-dense cytoplasmic inclusions (Fig. 6A). The contents of these electron-dense cytoplasmic vesicles consisted of lamellar material that resembled lipofuscin, a lipid substance with auto-fluorescence properties that has been shown to accumulate with aging in the lysosomes of all vertebrates. Neither the increase inside scatter nor the appearance of lipofuscin granules was seen in AsPC-1 cells transfected with or without AdCA *mock* vector (Fig. 6B, C). Cytotoxic changes in TOB-induced AsPC-1 cells showed the degradation of autophagy.

3.7. Anti-tumorigenic effects of AdCAtob vector on AsPC-1 cell-derived tumors in nude mice: morphological findings of tumors treated with AdCAtob vector

Pancreatic cancer peritonitis model was established in nude mice using ip injection of AsPC-1 cells. Four days after the ip injection of AsPC-1 cells, the mice were ip-injected with AdCA*tob* (50×10^6 or 150×10^6 pfu/0.5 ml/day, from day 5 to day 9).

Bloody ascites and multiple tumor nodules were seen at the mesothelium after 16 days of ip injection of 2, 5 and 10×10^6 AsPC-1 cells. We designed our initial experiments to determine whether *in vivo* AdCA*tob*-mediated gene transfer would affect the formation of pancreatic cancer peritonitis after implantation of cancer cells into the abdominal cavity. Peritoneal injection of AdCA*tob* suppressed tumor nodule formation in the abdominal cavity compared with the non-treated group (Fig. 7). Several tumor nodule formations were observed in AdCA*lacZ*-treated mice. Bloody ascites was not seen in either AdCA*tob or* AdCA*lacZ*-treated mice (Table 1).

3.8. Pathological findings of tumor treated with AdCAtob vector: adenovirus-mediated tob expression in vivo

Only one tumor nodule was recognized in the abdominal cavity of AdCA*tob* (50×10^6 pfu)-treated groups, and not found in that of 150×10^6 pfu groups. The tumor continued to express TOB with staining by anti-TOB monoclonal antibody, 4B1 (Fig. 8A). On the other hand, the jejunum, mesothelium, acinal gland and pancreatic islets of Langerhans did not show the expression of exogenous TOB with AdCA*tob* transfection (Fig. 8B). AsPC-1 cells expressing exogenous *tob* mRNA were enlarged and megakaryocytic with characteristics resembling those of senescent cells. These results suggest that our adenovirus-mediated *tob* gene therapy was applicable for the specific and efficient treatment of pancreatic cancer peritonitis.

Please cite this article in press as: Yanagie H et al., Tumor growth suppression by adenovirus-mediated introduction of a cell growth suppressing gene *tob* in a pancreatic cancer model, Biomed Pharmacother (2008), doi:10.1016/j.biopha.2008.04.010

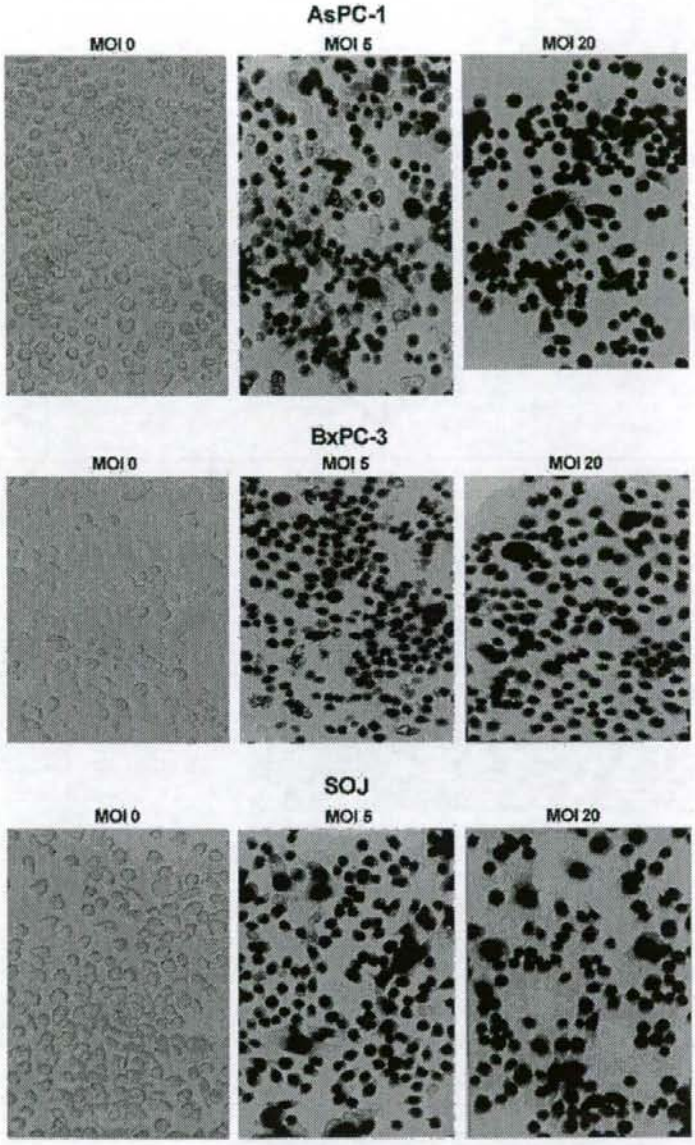

Fig. 2. Transduction efficiency of adenovirus in cancer cells *in vitro*. Optimal MOI for adenovirus-mediated gene transduction without virulence was determined in pancreatic cancer cells with control viral vector AdCA*lacZ*. AsPC-1, BxPC-3 and SOJ cells were plated on 24-well plates and transfected with AdCA*lacZ* at MOI of 0, 5, and 20. Forty-eight hours later, cells were fixed and stained with x-gal to demonstrate *lacZ* gene expression. The magnification of all photographs is ×400. No stained cells were detected at MOI 0 in the left panels, and increased transduction of *lacZ* in the right two panels of each cell line.

4. Discussion

The development of gene transfer technologies has provided new possibilities for the treatment of malignancies. Adenovirus vector systems that can produce high titers of viruses capable of efficient expression in target cells can deliver exogenous genes into a variety of cells and tissues.

Matsuda et al. reported that 185 kDa protein immunoreactive to anti-erbB-2 antibodies was detected in TOB immunoprecipitates, and a 45 kDa protein reactive to the anti-TOB antibodies was co-immunoprecipitated with $p185^{erbB-2}$, reciprocally [6,7]. TOB physically interacts with the *c-erbB-2* gene product. Exogenously expressed TOB is able to suppress the growth of NIH3T3 cells, and delivers growth inhibitory signals. These findings raise the possibility that the *tob* is a tumor suppressor gene [6,15]. Inspection of the deduced amino acid sequence of TOB revealed significant homologies (40.6%) to the BTG-1 anti-proliferative gene

Please cite this article in press as: Yanagie H et al., Tumor growth suppression by adenovirus-mediated introduction of a cell growth suppressing gene *tob* in a pancreatic cancer model, Biomed Pharmacother (2008), doi:10.1016/j.biopha.2008.04.010

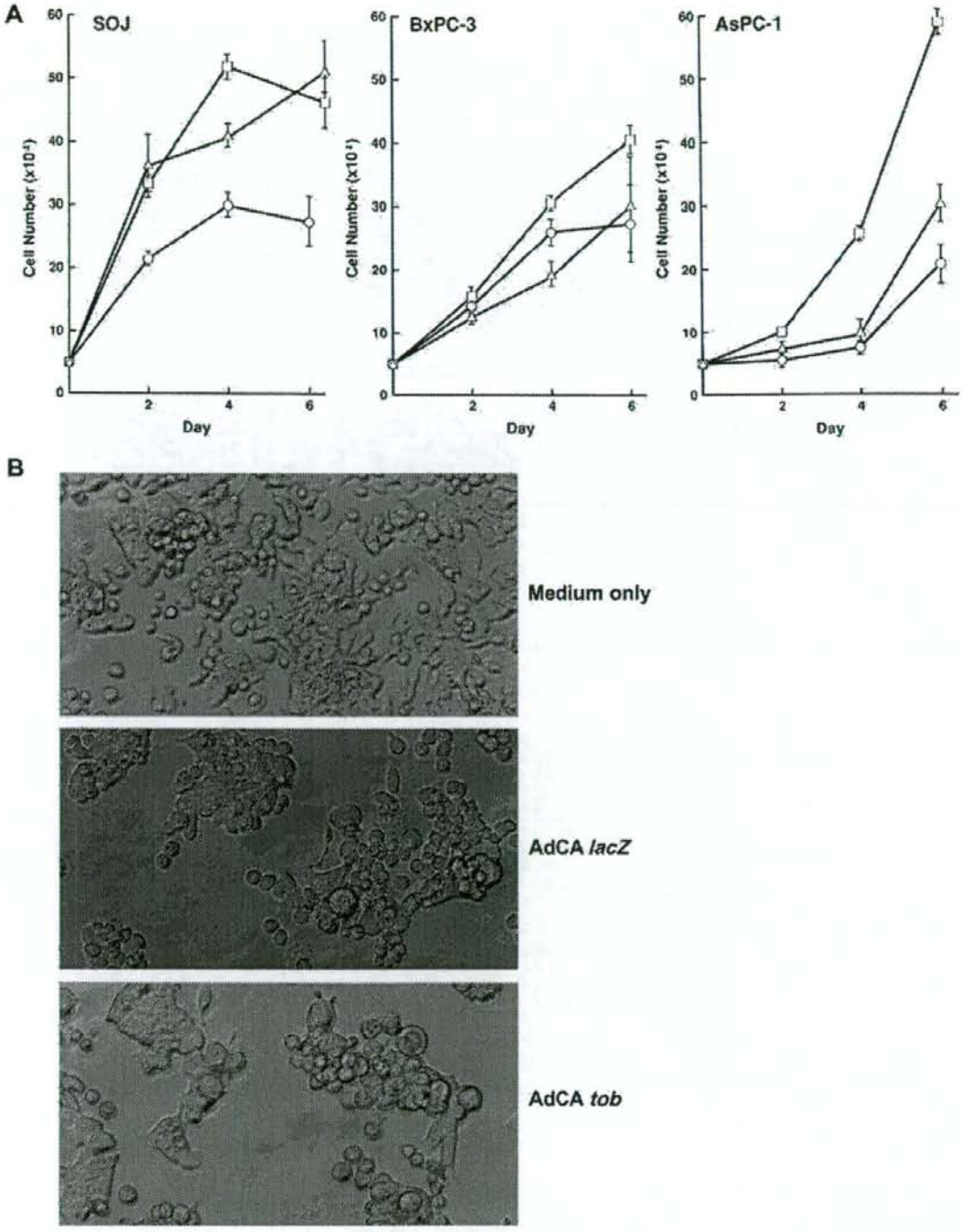

Fig. 3. (A) Tumor suppressor effect of the *tob* gene AsPC-1, BxPC-3, and SOJ cell lines were transfected with AdCA*tob* (○) or AdCA*lacZ* (△) at an MOI of 20. Medium without adenovirus vector (□) is also shown as medium only. These cancer cells could be transfected with MOI 20 without adenoviral virulence. Live cells were counted on the indicated days after transfection. Results are the means ± SD of three independent experiments. (B) Morphologies of transfected AsPC-1 cells with AdCA*tob*, AdCA*lacZ*, medium only without adenovirus vector. Enlarged megakaryotic cells appeared with many granules in cytoplasm. Photograph magnification is ×400.

Please cite this article in press as: Yanagie H et al., Tumor growth suppression by adenovirus-mediated introduction of a cell growth suppressing gene *tob* in a pancreatic cancer model, Biomed Pharmacother (2008), doi:10.1016/j.biopha.2008.04.010

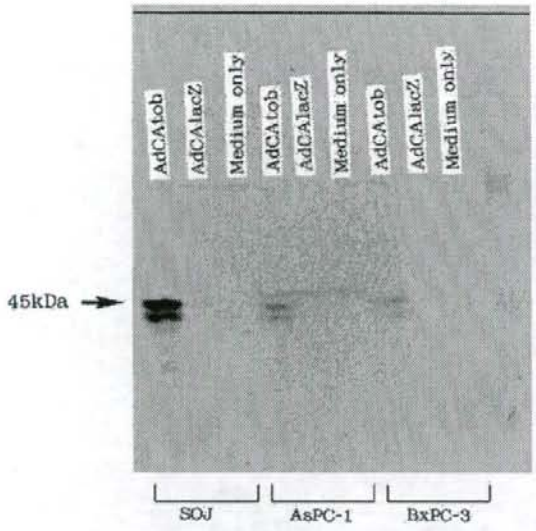

Fig. 4. Western blot analysis of lysates of pancreatic cancer cell lines after transfection of AdCA*lacZ* or AdCA*tob* using the anti-TOB monoclonal antibody Transfected adenovirus vectors are indicated above lanes. Cancer cells are indicated below lanes. Arrow on the left side of gel indicates 45 kDa band specific to exogenous TOB. Band higher than 45 kDa indicates endogenous TOB expressed in AsPC-1 cells.

product and to the PC 3 (BTG-2) gene product at its amino-terminal half. Both BTG-1 and BTG-2, having the significant homologies to TOB, suppress cell growth, and perform cell cycle control [8,9]. ANA, belonging to the anti-proliferative TOB family, interacts with CCR transcription factor-associated protein Cafl [16,17].

NIH3T3 cells expressing exogenous *tob* mRNA were enlarged and showed swollen nuclei with many granules in the cytoplasm. The characteristics resembled those of senescent cells. Evidence of senescence change were the accumulation of lipofuscin granules, an ultrastructural change associated with aging, and flattened enlarged cell morphology. TOB exhibits anti-proliferative activity when the level of its expression is elevated and/or deregulated. The interaction of TOB with *c-erbB-2* gene products was suggested to occur through the carboxyl-terminal half of TOB. Exogenously expressed TOB also exhibits anti-proliferative activity. Protein-tyrosine kinase receptors induce the expression of G1 cyclins, which in turn interact with and activate CDK family proteins, resulting in the phosphorylation of Rb protein. It is necessary to examine whether protein-tyrosine kinases other than $p185^{erbB-2}$ could also interact with TOB in the proliferative signal transduction of cancer cells. Expression of BTG-1 is high in G0/G1 phases of the cell cycle and is down regulated when the cells enter the growth cycle, suggesting that the gene product is inhibitory to G0/G1 progression. A forced expression of exogenous BTG-1 in NIH3T3 cells resulted in the suppression of cell growth [8]. The BTG-1 gene is 60% homologous to PC3, an immediate early gene induced by nerve growth factor in rat PC12 cells. Rouault et al. named PC3 as BTG-2, and have reported that BTG-2 expression is induced through a p53-dependent mechanism and the function may be relevant to cell cycle control and cellular response to DNA damage [9].

Yoshida et al. had reported that *tob* is a member of anti-proliferative family genes. Mice lacking *tob* are prone to spontaneous formation of tumors. The occurrence rate of diethylnitrosamine-induced liver tumors is higher in $tob^{-/-}$ mice than in wild-type mice. $TOB^{-/-}$ $p53^{-/-}$ mice show accelerated tumor formation in comparison with single null mice. Expression of cyclin D1 mRNA is increased in the absence of and reduced by TOB [18]. Suzuki et al. had reported that TOB inhibits cell growth by suppressing cyclin D1 expression, which is canceled by Erk1- and Erk2-mediated TOB phosphorylation. TOB is critically involved in the control of early G1 progression [19]. Iwanaga et al. reported

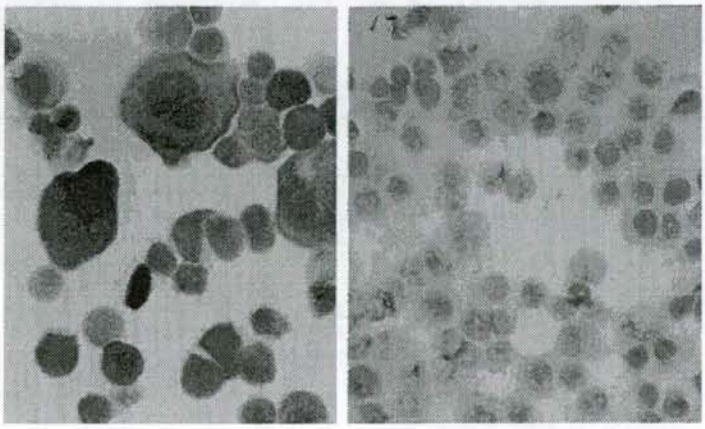

Fig. 5. AdCA*tob* vector-mediated *tob* expression *in vitro* AsPC-1 cells (50×10^3) were transfected with AdCA*tob* vector (MOI 20). After 72 h, cells were collected and stained with anti-TOB monoclonal antibody 4B1 by peroxidase immunostaining in order to determine the expression of TOB protein. Photograph magnification is ×400. Left: transfected cells were well stained. Right: non-treated naïve cells.

Please cite this article in press as: Yanagie H et al., Tumor growth suppression by adenovirus-mediated introduction of a cell growth suppressing gene *tob* in a pancreatic cancer model, Biomed Pharmacother (2008), doi:10.1016/j.biopha.2008.04.010

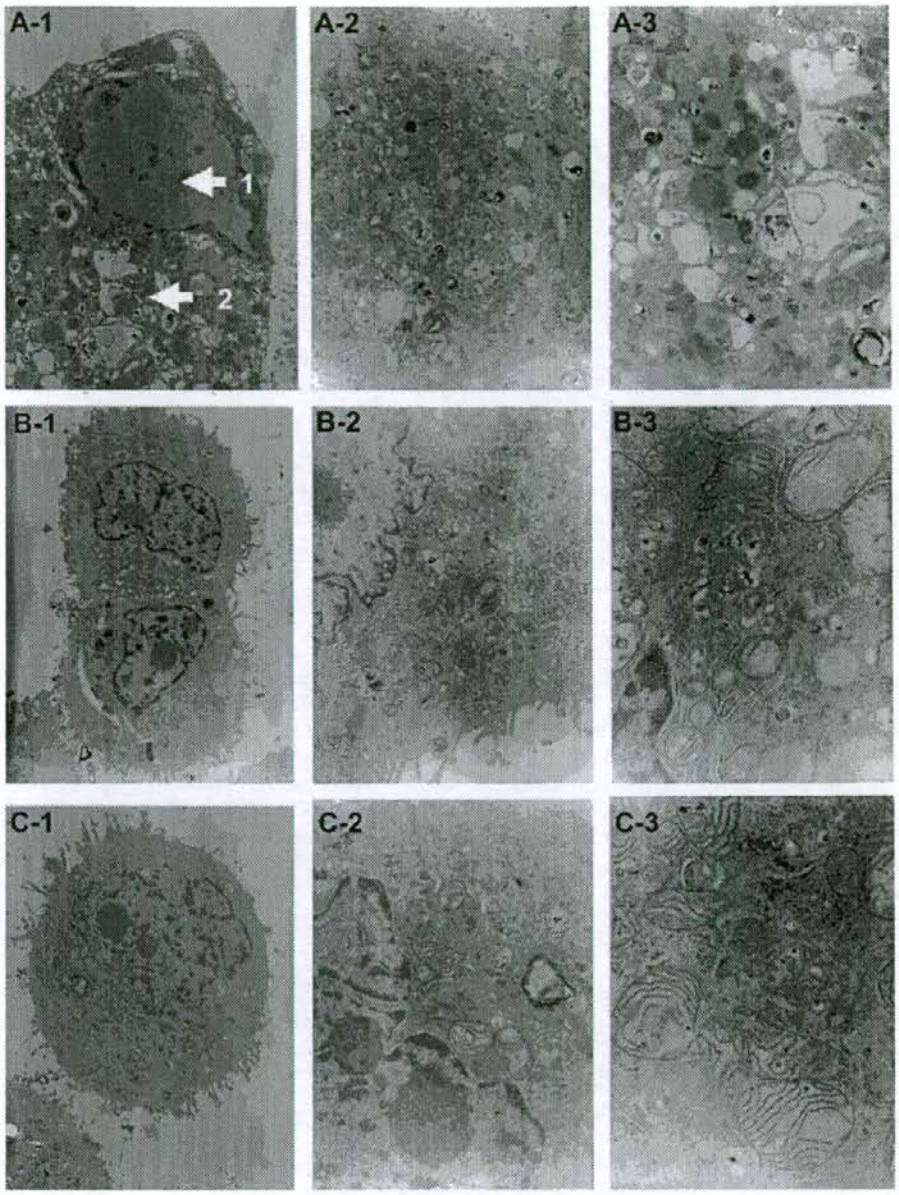

Fig. 6. Cytotoxic effect on AsPC-1 with *tob* expression by AdCA*tob* vector on electron microscopy. (A) AdCA*tob* transfectant (MOI 100), (B) AdCA *mock* transfectant (MOI 100), (C) Non-treated control. (A) AdCA*tob* transfectant (MOI 100) showed degradation of nucleus (arrowhead 1), many autophagosomes and electron-dense cytoplasmic inclusions (arrowhead 2). The contents of these vesicles consisted of lamellar material that resembled lipofuscin, a lipid substance with auto-fluorescence properties. (B) AdCA *mock* transfectant (MOI 100) showed irregular-shaped nucleus, enlargements and deformities of mitochondria, increase of endoplasmic reticulum and lysosome vesicles. No increase of lipofuscin granules. (C) Non-treated control showed irregular-shaped nucleus, enlargement of mitochondria, increase of endoplasmic reticulum. Several autophagosomes were seen in cells treated with AdCA *mock* and non-treated cells, but increase of autophagosomes were recognized in cells treated with AdCA*tob*. There was neither an increase of inside scatter nor the appearance of lipofuscin granules. A-1, B-1, and C-1 are low magnification of the photograph (×5000), A-2, B-2, and C-2 are high magnification of the photograph (×8000), and A-3, B-3, and C-3 are high magnification of the photograph (×15,000).

Please cite this article in press as: Yanagie H et al., Tumor growth suppression by adenovirus-mediated introduction of a cell growth suppressing gene *tob* in a pancreatic cancer model, Biomed Pharmacother (2008), doi:10.1016/j.biopha.2008.04.010

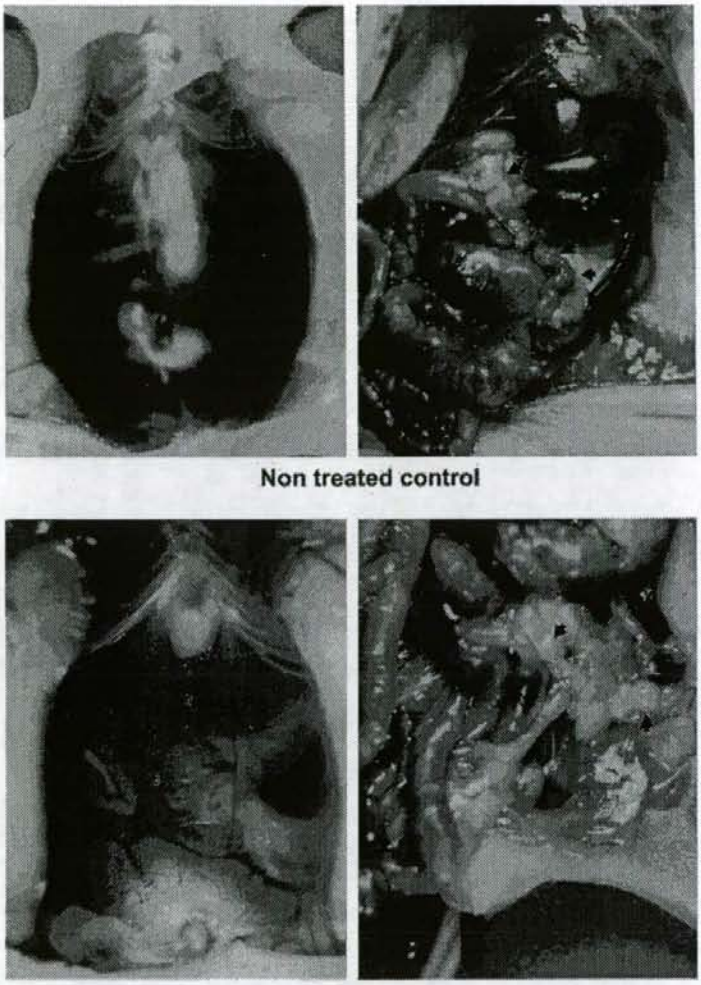

Fig. 7. Tumor growth suppression of cancer peritonitis model with peritoneal AdCA*tob* transfection. Bloody ascites and tumor growth suppression in the abdominal cavity disappeared with viral *tob* expression. (A). Non-treated control; Bloody ascites (Left) and multiple tumor nodules (Right) were seen at the mesentery after 16 days of 2×10^6 ip injection of AsPC-1 cells. (B). AdCA*tob*-treated; mice underwent ip injections of AdCA*tob* (1.5×10^8 pfu/0.2 ml/day, from day 5 to day 9) after 4 days of ip injection of 2×10^6 AsPC-1 cells. Peritoneal injections of AdCA*tob* suppressed tumor nodule formation in the abdominal cavity compared with the non-treated group (Right). Bloody ascites was not seen in AdCA*tob*-treated mice (Left).

that the phosphorylated and inactive form of TOB was detected in 76% of cancer tissues of adenocarcinoma patients, but not in normal alveolar epithelial cells [20]. Cho et al. reported that phosphorylation of myristoylated alanine-rich C kinase substrate, MARCKS, removes TOB from ErbB-2 by increasing its binding affinity with TOB, and thereby activates ErbB-2-mediated signal transduction [21]. TOB phosphorylation contributes to the progression of papillary carcinoma of the thyroid, especially in the later phase through cancellation of its anti-proliferative function [22]. Exogenous overexpression of TOB family proteins suppresses cell proliferation. Mutation in the nuclear localization signal sequence of TOB affects its nuclear localization and impairs anti-proliferative activity [23,24]. ERK phosphorylation negatively regulates the anti-proliferative function of TOB [25]. Sasajima et al. reported that the BTG/TOB family was degraded by the ubiquitin-proteasome system [26].

We evaluated the expression of *tob* mRNA and gene product in pancreatic cancer cell lines, AsPC-1, BxPC-3, and SOJ with or without *tob* transfection. The *tob* mRNA was expressed in all pancreatic cancer cell lines, and the level of *tob* mRNA of AsPC-1 cells was strongest among them. The *tob* mRNA

Please cite this article in press as: Yanagie H et al., Tumor growth suppression by adenovirus-mediated introduction of a cell growth suppressing gene *tob* in a pancreatic cancer model, Biomed Pharmacother (2008), doi:10.1016/j.biopha.2008.04.010

Table 1
Inhibition of the formation of pancreatic cancer peritonitis with Adeno-virus mediated *tob* gene transfer *in vivo*

Treatment group	Tumor nodules		Ascites	
AdCA*tob* (1.5×10^8 pfu) ($n=4$)	–	(0/4)	±	Serous
AdCA*tob* (5×10^7 pfu) ($n=3$)	+	(1/3)	±	Serous
AdCA*lacZ* (1.5×10^8 pfu) ($n=3$)	+	(2/3)	±	Serous
AdCA*lacZ* (5×10^7 pfu) ($n=3$)	+	(2/3)	+~++	Turbid
Non-treated (1.5×10^8 pfu) ($n=3$)	+++	(3/3)	+++	Bloody

Despite the observed heterogeneity for individual animals, a significant tumor growth inhibitory effects of AdCA*tob* has been noted.

expression was increased in correlation with erbB-2 mRNA expression in AsPC-1 and BxPC-3 cells, but the endogenous *tob* gene product is not increased in these cells.

Overexpression of erbB-2 and EGF-R protein was observed in pancreatic cancer cells, so the suppressive effect of endogenous TOB could be impaired by the passage of protein-tyrosine kinases as $p185^{erbB-2}$. We prepared adenoviral vector containing *tob* cDNA (AdCA*tob*). AdCA*tob* was transfected and expanded in 293 cells. The titer of the vector was 350×10^6 pfu/ml. Monitoring the viability of pancreatic cancer cells transfected with adenoviral vector containing the *lacZ* gene revealed that these cancer cells were able to be transfected with MOI 20 without adenoviral toxicity. Growth

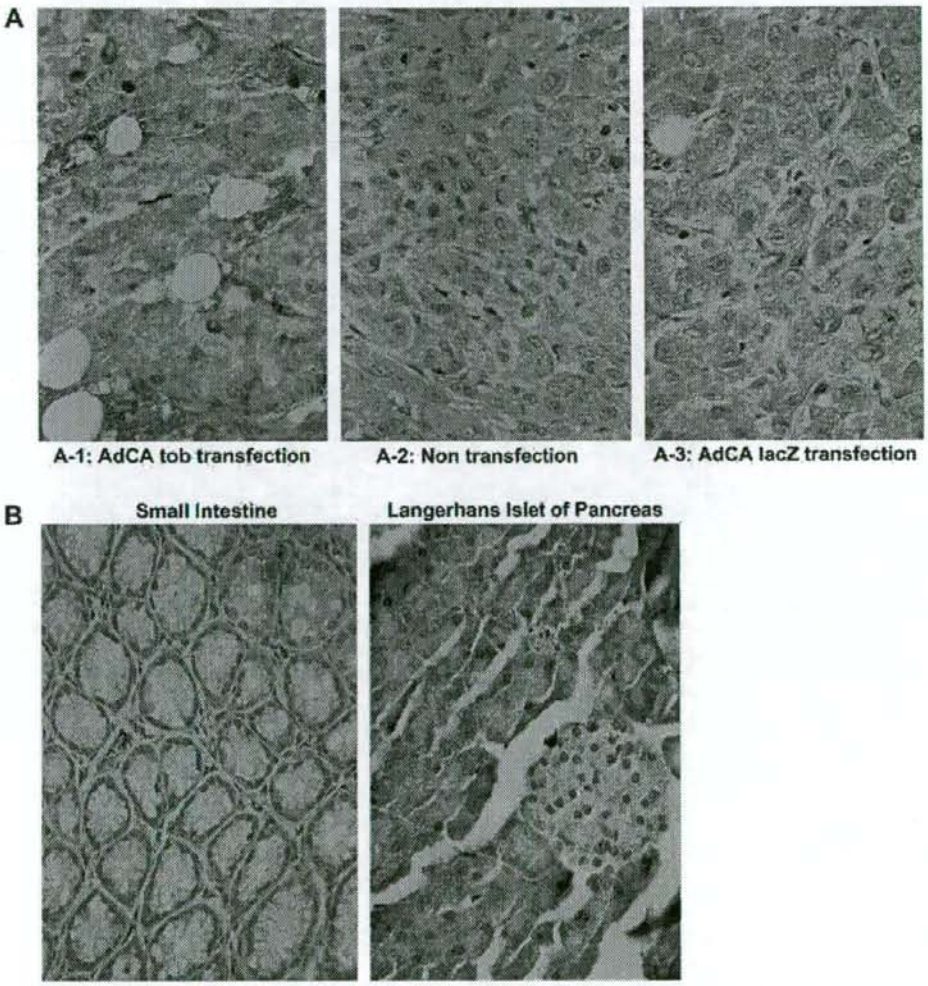

Fig. 8. Pathological findings of tumor treated with AdCA*tob* vector *in vivo*. Only one tumor nodule was recognized in the abdominal cavity in the AdCA*tob* (5×10^7 pfu)-treated group, and not found in 1.5×10^8 pfu groups. The tumor continued to express TOB with staining by anti-TOB monoclonal antibody 4B1 (A-1). Tumors of non-treated control (A-2) and AdCA*lacZ* (A-3)-transfected groups showed only a few endogenous TOB. The jejunum (B-1), mesothelium, acinal gland and pancreatic islets of Langerhans (B-2) did not show the expression of exogenous TOB with AdCA*tob* transfection.

Please cite this article in press as: Yanagie H et al., Tumor growth suppression by adenovirus-mediated introduction of a cell growth suppressing gene *tob* in a pancreatic cancer model, Biomed Pharmacother (2008), doi:10.1016/j.biopha.2008.04.010

suppression with transfection of AdCA*tob* was shown in SOJ and AsPC-1 cell lines according to *tob* expression. We evaluated the tumor-suppressing effects of AdCA*tob* in pancreatic cancer cell lines. SOJ and AsPC-1 cell lines transfected by AdCA*tob* showed growth suppression. Significant suppression was shown in SOJ cell lines after the overexpression of TOB. These results suggest that the recombinant adenovirus vector containing the *tob* gene is a useful candidate for anti-tumor gene therapy, and could be applied for cancer peritonitis. AsPC-1 cells expressing the exogenous *tob* were enlarged and megakaryocytic with characteristics resembling those of senescent cells.

We also found that TOB-overexpressing AsPC-1 cells showed degradation of the nucleus and many autophagosomes and electron-dense cytoplasmic inclusions. One cancer cytotoxic mechanism is based on autophagy. Autophagy is a cellular degradation pathway for the clearance of damaged or superfluous proteins and organelles [27,28], and a survival pathway required for cellular viability during starvation; however, if it proceeds to completion, autophagy can lead to cell death. Autophagy has emerged as a homeostatic mechanism regulating the turnover of long-lived or damaged proteins and organelles, and buffering metabolic stress under conditions of nutrient deprivation by recycling intracellular constituents. Autophagy is also a form of cell death, when allowed to proceed to excessive levels and when apoptosis-defective cells are triggered to die. It has been thought that autophagy may play an active role in programmed cell death [29]. We had observed autophagic conformation by the formulation of autophagosomes and localization of GFP-LC3 on the cytotoxicity of human pancreatic cancer cells treated with polyoxomolybdates (PM-17) [30]. Faiy et al. indicated that quercetin induced autophagy specifically in Ha-RAS-transformed cells [31]. They had reported that flavonoid quercetin drastically reduces the half-life of oncogenic Ras, and Ras protein levels in cell lines expressing oncogenic Ras proteins. Quercetin induces autophagic processes in Ha-RAS-transformed cells. Microtubule-associated protein light chain 3 (LC3) protein is localized in autophagosomes and autolysosomes membranes after processing in quercetin-treated cancer cell lines.

In this report, we also prepared pancreatic cancer peritonitis models using ip injection of AsPC-1 cells. In this model, bloody ascites and multiple tumor nodules were seen at the mesentery after 16 ip days. We administered ip injection of AdCA*tob* to mice bearing pancreatic cancer peritonitis. Tumor growth was suppressed 10 days after ip injections of AdCA*tob* compared to the control group. Our new model of gene therapy for pancreatic cancer by AdCA*tob* in the first week induced significant tumor reduction and complete tumor regression. There was no tumor nodule in the abdomen and no bloody ascites. AdCA*tob* has shown no significant toxic effect on untransformed cells. AdCA*tob* treatment produced significant growth inhibition both *in vivo* and *in vitro*.

Overexpression of wt p53 triggered a short-term cellular response leading to irreversible growth arrest and senescence [32–34]. The commitment to senescence became irreversible with in 48–72 h and no longer required p53 expression. A number of studies utilizing adenoviral or retroviral vectors have evaluated the anti-proliferative and anti-tumorigenic potential of restoration of wild-type p53 in *in vitro* as well as *in vivo* animal models of cancer [35–40]. Nielsen et al. reported that ip injection of AdCMV*wt p53* resulted in reducing the tumor burden of SK-OV-3 ovarian cancer *in vivo* [2]. We also performed ip injections of AdCMV*wt p53* (5×10^7 pfu/day, from day 5 to day 9) after 4 days of ip inoculation of AsPC-1 cells, and tumor growth was suppressed 10 days after ip injections of AdCMV*wt p53* (data not shown). Tumor suppressor gene *p53* includes the regulation of G1-associated cell growth inhibition, maintenance of genomic integrity, control of the apoptotic pathway, and regulation of inhibitors of angiogenesis. Consequently, reconstituting the normal p53 function in tumor cells with defective p53 via introduction of the *wt p53* gene may have therapeutic utility [41,42].

It has been known that the adenovirus vector-mediated gene transfer system has several limitations for *in vivo* application, including transient expression of transferred gene and immunogenic response of the host against adenovirus. As an extension of this study, we are now evaluating the *tob* gene therapeutic potential with a cationic liposomal delivery system to a pancreatic cancer model. Injection of the AdCA*tob* vector provides significant growth inhibition of tumor progression, and our study offers strong support for the gene therapeutic potential of this vector in human pancreatic cancer peritonitis. Continuous progression of these investigations in the future will be necessary for the successful development of a new treatment modality for clinical trials of gene therapy for metastatic pancreatic cancer.

Acknowledgements

The authors are grateful to Professor Alistair Renwick, Institute of Health and Community Medicine, University of Malaysia Sarawak, for comments on the manuscript. This work was supported in part by a Grant-in-Aid for Scientific Research from the Ministry of Education, Science, Sport and Culture, Japan (No. 15390389 and 15659308 to Hironobu Yanagie), a Grant from the Sato Memorial Foundation for Cancer Research (to Hironobu Yanagie), and a Grant from the Foundation for the Promotional of Cancer Research in Japan (to Hironobu Yanagie).

References

[1] Reyes G, Villanueva A, Garcia C, Sancho FJ, Piulats J, Lluis F, et al. Orthotopic xenografts of human pancreatic carcinomas acquire genetic aberrations during dissemination in nude mice. Cancer Res 1996;56:5713–9.

[2] Nielsen LL, Gurnani M, Syed J, Dell J, Hartman B, Cartwright M, et al. Recombinant E1-deleted adenovirus-mediated gene therapy for cancer: efficacy studies with p53 tumor suppressor gene and liver histology in tumor xenografts models. Hum Gene Ther 1998;9:681–94.

[3] Fueyo J, Gomez-Manzano C, Yung WKA, Liu TJ, Alemany R, McDonnell TJ, et al. Overexpression of E2F-1 in glioma triggers apoptosis and suppresses tumor growth in vitro and in vivo. Nat Med 1998;4:685–90.

[4] Iqbal-Ahmed CM, Sugarman BJ, Johnson DE, Bookstein RE, Saha DP, Nagabhushan TL, et al. *In vivo* tumor suppression by adenovirus-mediated Interferon α2b gene therapy. Hum Gene Ther 1999;10:77–84.

[5] Kaneko S, Hallenbeck P, Kotani T, Nakabayashi H, McGarrity G, Tamaoki T, et al. Adenovirus-mediated gene therapy of hepatocellular carcinoma using cancer-specific gene expression. Cancer Res 1995;55: 5283–7.

[6] Matsuda S, Kawamura J, Ohsugi M, Yoshida M, Emi M, Nakamura Y, et al. Tob, a novel protein that interacts with p185 erbB2, is associated with anti-proliferative activity. Oncogene 1996;12:705–13.

[7] Akiyama T, Matsuda S, Namba Y, Saito T, Toyoshima K, Yamamoto T. The transforming potential of the c-erbB-2 protein is regulated by its autophosphorylation at the carboxyl-terminal domain. Mol Cell Biol 1991; 11:833–42.

[8] Rouault JP, Rimokh R, Tessa C, Paranhos G, Ffrench M, Duret L, et al. BTG-1, a member of a new family of antiproliferative genes. EMBO J 1992;11:1663–70.

[9] Rouault JP, Falette N, Guehenneux F, Guillot C, Rimokh R, Wang Q, et al. Identification of BTG2, an antiproliferative p53-dependent component of the DNA damage cellular response pathway. Nat Genet 1996;14: 482–6.

[10] Rouault JP, Samarut C, Duret L, Tessa C, Samarut J, Magaud JP. Sequence analysis reveals that the BTG-1 anti-proliferative gene is conserved throughout evolution in its coding and 3' non-coding regions. Gene 1993;129:303–6.

[11] Kanai F, Lan KH, Shiratori Y, Tanaka T, Ohashi M, Okudaira T, et al. *In vivo* gene therapy for a-fetoprotein-producing hepatocellular carcinoma by adenovirus-mediated transfer of cytosine deaminase gene. Cancer Res 1997;57:461–5.

[12] Tanaka T, Kanai F, Okabe S, Yoshoda Y, Wakimoto H, Hamada H, et al. Adenovirus-mediated prodrug gene therapy for carcinoembryonic antigen-producing human gastric carcinoma cells *in vitro*. Cancer Res 1996;56:1341–5.

[13] Kanegae Y, Lee G, Sato Y, Tanaka M, Nakai M, Sasaki T, et al. Efficient gene activation in mammalian cells by using recombinant adenovirus expressing site-specific Cre recombinase. Nucleic Acids Res 1995;23: 3816–21.

[14] Zenilman ME, Magnuson TH, Perfetti R, Chen J, Shuldiner AR. Pancreatic *reg* gene expression is inhibited during cellular differentiation. Ann Surg 1997;225:327–32.

[15] Yoshida Y, Matsuda S, Yamamoto T. Cloning characterization of the mouse *tob* gene. Gene 1997;191:109–13.

[16] Yoshida Y, Matsuda S, Ikematsu N, Kawamura-Tsuzuku J, Inazawa J, Umemori H, et al. ANA, a novel member of Tob/BTG-1 family, is expressed in the ventricular zone of the developing central nervous system. Oncogene 1998;16:2687–93.

[17] Yoshida Y, Hosoda E, Nakamura T, Yamamoto T. Association of ANA, a member of the antiproliferative Tob family proteins, with a Caf1 component of the CCR4 transcriptional regulatory complex. Jpn J Cancer Res 2001;92:592–6.

[18] Yoshida Y, Nakamura T, Komoda M, Satoh H, Suzuki T, Tsuzuki KJ, et al. Mice lacking a transcriptional co-repressor Tob are predisposed to cancer. Genes & Dev 2003;17:1201–6.

[19] Suzuki T, K-Tsuzuku J, Ajima R, Nakamura T, Yoshida Y, Yamamoto T. Phosphorylation of three regulatory serines of Tob by Erk1 and Erk2 is required for Ras-mediated cell proliferation and transformation. Genes Dev 2002;16(11):1356–70.

[20] Iwanaga K, Sueoka N, Sato A, Sakuragi T, Sakao Y, Tominaga M, et al. Alteration of expression or phosphorylation status of tob, a novel tumor suppressor gene product, is an early event in lung cancer. Cancer Lett 2003;202:71–9.

[21] Cho SJ, La M, Ahn JK, Meadows GG, Joe CO. Tob-mediated cross-talk between MARCKS phosphorylation and ErbB-2 activation. Biochem Biophy Res Comm 2001;283:273–7.

[22] Ito Y, Suzuki T, Yoshida H, Tomoda C, Uruno T, Takamura Y, et al. Phosphorylation and inactivation of Tob contributes to the progression of papillary carcinoma of the thyroid. Cancer Lett 2005;220:237–42.

[23] Kawamura-Tsuzuku J, Suzuki T, Yoshida Y, Yamamoto T. Nuclear localization of Tob is important for regulation of its antiproliferative activity. Oncogene 2004;23:6630–8.

[24] Maekawa M, Yamamoto T, Nishida E. Regulation of subcellular localization of the antiproliferative protein Tob by its nuclear export signal and bipartite nuclear localization signal sequences. Exp Cell Res 2004; 295:59–65.

[25] Maekawa M, Nishida E, Tanoue T. Identification of the Anti-proliferative protein Tob as a MAPK substrate. J Biol Chem 2002;277:37783–7.

[26] Sasajima H, Nakagawa K, Yokosawa H. Antiproliferative proteins of the BTG/Tob family are degraded by the ubiquitin-proteasome system. Eur J Biochem 2002;269:3596–604.

[27] Omodeizorini A. Considerations on primary carcinomatous caverns of the lung. Possibility of the intervention of a phenomenon of "Autophagia of the neoplastic cells". Riforma Med 1964;78:533–50 [in Italian].

[28] Mathew R, Karantza-Wadsworth V, White E. Role of autophagy in cancer. Nat Rev Cancer 2007 Dec;7(12):961–7.

[29] Karantza-Wadsworth Vassiliki, White Eileen. Role of autophagy in breast cancer. Autophagy 2007;3(6):610–3.

[30] Ogata A, Yanagie H, Ishikawa E, Morishita Y, Mitsui S, Yamashita A, et al. Antitumour effect of polyoxomolybdates: induction of apoptotic cell death and autophagy in *in vitro* and *in vivo* models. Br J Cancer 2008;98(2):399–409.

[31] Psahoulia Faiy H, Moumtzi Sophy, Roberts Michael L, Sasazuki Takehiko, Shirasawa Senji, Pintzas Alexander. Quercetin mediates preferential degradation of oncogenic Ras and causes autophagy in Ha-RAS- transformed human colon cells. Carcinogenesis 2007;28: 1021–31.

[32] Asgari K, Sesterhenn IA, Mcleod DG, Cowan K, Moul JW, Seth P. Inhibition of the growth of pre-established subcutaneous tumor nodules of human prostate cancer cells by single injection of the recombinant adenovirus p53 expression vector. Int J Cancer 1997;71:377–82.

[33] Sugrue MM, Shin DY, Lee SW, Aaronson SA. Wild-type p53 triggers a rapid senescence program in human tumor cells lacking functional p53. Proc Natl Acad Sci U S A 1997;94:9648–53.

[34] Hamada K, Alemany R, Zhang WW, Hittelman WN, Lotan R, Roth JA, et al. Adenovirus-mediated transfer of a wild-type *p53* gene and induction of apoptosis in cervical cancer. Cancer Res 1996;56:3047–54.

[35] Eastham JA, Hall SJ, Sehgal I, Wang J, Timme TL, Yang G, et al. *In vivo* gene therapy with p53 or p21 adenovirus for prostate cancer. Cancer Res 1995;55:5151–5.

[36] Yang C, Cirielli C, Capogrossi C, Passantini A. Adenovirus-mediated wild-type p53 expression induces apoptosis and suppresses tumorigenesis of prostatic tumor cells. Cancer Res 1995;55:4210–3.

[37] Clayman GL, El-Naggar AK, Roth JA, Zhang WW, Goepfect H, Taylor DL, et al. *In vivo* molecular therapy with p53 adenovirus for microscopic residual head and neck squamous carcinoma. Cancer Res 1995;55:1–6.

[38] Graber HU, Friess H, Kaufmann B, Willi D, Zimmermann A, Korc M, et al. ErbB-4 mRNA expression is decreased in non-metastatic pancreatic cancer. Int J Cancer 1999;84:24–7.

[39] Putzer BM, Bramson JL, Addison CL, Hitt M, Siegel PM, Muller WJ, et al. Combination therapy with Interleukin-2 and wild-type p53 expressed by adenoviral vectors potentiates tumor regression in a murine model of breast cancer. Hum Gene Ther 1998;9:707–18.

[40] Sandig V, Brand K, Herwig S, Lukas J, Bartek J, Strauss M. Adenovirally transferred $p16^{INK4/CDKN2}$ and p53 genes cooperate to induce apoptotic tumor cell death. Nat Med 1997;3:313–9.

[41] Harris MP, Sutjipto S, Wills KN, Hancock W, Cornell D, Johnson DE, et al. Adenovirus-mediated *p53* gene transfer inhibits growth of human tumor cells expressing mutant p53 protein. Cancer Gene Ther 1996;3: 121–30.

[42] Harada N, Gansauge S, Gansauge F, Gause H, Shimoyama S, Imaizumi T, et al. Nuclear accumulation of p53 correlates significantly with clinical features and inversely with the expression of the cyclin-dependent kinase inhibitor$^{WAF-1/CIP1}$ in pancreatic cancer. Br J Cancer 1997;76:299–305.

Please cite this article in press as: Yanagie H et al., Tumor growth suppression by adenovirus-mediated introduction of a cell growth suppressing gene *tob* in a pancreatic cancer model, Biomed Pharmacother (2008), doi:10.1016/j.biopha.2008.04.010

ELSEVIER

Experimental Hematology

Experimental Hematology 2008;36:1634–1641

Bioluminescent evaluation of the therapeutic effects of total body irradiation in a murine hematological malignancy model

Yusuke Inoue[a], Kiyoko Izawa[b], Shigeru Kiryu[c], Seiichiro Kobayashi[b], Arinobu Tojo[b], and Kuni Ohtomo[c]

[a]*Department of Radiology, Institute of Medical Science, University of Tokyo, Tokyo, Japan;* [b]*Division of Molecular Therapy, Advanced Clinical Research Center, Institute of Medical Science, University of Tokyo, Tokyo, Japan;* [c]*Department of Radiology, Graduate School of Medicine, University of Tokyo, Tokyo, Japan*

(Received 28 June 2008; revised 18 August 2008; accepted 20 August 2008)

Objective. **We investigated the utility of in vivo bioluminescence imaging (BLI) in assessing the therapeutic effects of total body irradiation (TBI) in a murine hematological malignancy model.**

Materials and Methods. **The suspension of Ba/F3 cells transduced with firefly luciferase and p190 BCR-ABL genes was exposed to ionizing radiation, and viable cell numbers and bioluminescent signals were measured serially. Mice intravenously inoculated with the cells underwent TBI at various doses. In vivo BLI was performed repeatedly until spontaneous death, and whole-body bioluminescence signals were determined as an indicator of whole-body tumor burden.**

Results. **In the cell culture study, bioluminescence signals generally reflected viable cell numbers, despite some overestimation immediately after irradiation. Sublethal TBI in mice transiently depressed the increase in whole-body signals and prolonged survival. Spontaneous death occurred at similar signal levels regardless of radiation dose. A significant negative correlation was found between survival and whole-body signal early after TBI. Significant dose dependence was demonstrated for both survival and signal increase early after TBI and was more evident for signal increase. Lethally irradiated mice without bone marrow transplantation died while showing weak signals. In mice receiving lethal TBI and syngeneic bone marrow transplantation, signal reduction and prolongation of survival were prominent, and whole-body signals at death were similar to those in nonirradiated or sublethally irradiated mice.**

Conclusion. **In vivo BLI allows longitudinal, quantitative evaluation of the response to TBI in mice of a hematological malignancy model. Antitumor effects can be assessed early and reliably using in vivo BLI.** **© 2008 ISEH - Society for Hematology and Stem Cells. Published by Elsevier Inc.**

In vivo bioluminescence imaging (BLI) allows noninvasive, whole-body evaluation of luciferase expression in intact small animals and is used increasingly to evaluate the effects of novel therapeutic strategies against malignant neoplasms [1,2]. For bioluminescent tumor monitoring, mice are inoculated with tumor model cells stably expressing firefly luciferase. Injection of the mice with D-luciferin, substrate for firefly luciferase, induces light emission from the cells, and images that reflect the amount and distribution of the inoculated cells can be acquired repeatedly in individual animals.

In vivo BLI has been applied to studies using animal models of hematological malignancies [3–8]. In hematological malignancy models, various organs, including bone marrow, lymph nodes, liver, and spleen may be involved and, because of the difficulty in assessing whole-body tumor burden, therapeutic effects are evaluated in conventional experiments primarily based on survival. However, in addition to the time-consuming nature of survival assessment, survival may be affected by various confounding factors other than the antitumor effects of the therapeutic intervention, and many animals are required to yield

Offprint requests to: Yusuke Inoue, MD, Department of Radiology, Institute of Medical Science, University of Tokyo, 4-6-1 Shirokanedai, Minato-ku, Tokyo 108-8639, Japan; E-mail: inoueys-tky@umin.ac.jp

0301-472X/08 $–see front matter. Copyright © 2008 ISEH - Society for Hematology and Stem Cells. Published by Elsevier Inc.
doi: 10.1016/j.exphem.2008.08.004

statistically relevant results. Deaths from tumor progression need to be discriminated from treatment-related or accidental deaths. Because of the limitations of survival assessment, in vivo BLI may be particularly beneficial for animal experiments of hematological malignancies.

It has been validated in various tumor models that the intensity of light signals determined from in vivo BLI reflects tumor burden quantitatively [9–18]. However, most studies have assessed the relationship between tumor size and BLI signal without therapeutic interventions, and validation studies concerning tumors after therapy are limited. Some studies have revealed discrepancies between tumor sizes and BLI signals in treated animals [17–19]. Although these discrepancies were attributed to BLI reflecting viable tumors selectively, whereas tumor size measurements are affected by necrotic or fibrotic components of the tumor and were interpreted as evidence of the superiority of BLI over size measurements, the reliability of BLI assessment of therapeutic efficacy and posttreatment regrowth has not been fully established.

Radiotherapy, including total body irradiation (TBI), plays an important role as a treatment option for hematological malignancies [20], and further improvements of treatment strategies, including optimization of radiation dose, schedule, and field design, use of a radiosensitizer or radioprotector, and combinations with other treatment modalities, are being pursued [21–24]. Animal experiments using in vivo BLI may aid such investigations. In this study, we evaluated in vitro relationships between viable cell number and luminescent intensity longitudinally after exposing luciferase-expressing cells of a hematological malignancy model to ionizing radiation. Moreover, mice inoculated intravenously with the cells underwent TBI at various doses with or without bone marrow transplantation (BMT). In vivo BLI was performed repeatedly until spontaneous death, and the effects of the different treatments were monitored in individual mice based on survival and BLI signals. The principal aim of this study was to determine the potential of in vivo BLI for assessment of the therapeutic efficacy of TBI in mice of a hematological malignancy model.

Materials and methods

Cell lines

The interleukin-3–dependent murine pro – B-cell line Ba/F3 was cotransfected with the firefly luciferase gene and the wild-type p190 BCR-ABL fusion gene using a retroviral method described previously [25]. Stable transfectants were selected, and the established cells were named Ba/F3-Luc/Wt cells. The cDNA encoding firefly luciferase was excised from the pGL3-basic vector (Promega, Madison, WI, USA), and the long terminal repeat (LTR) of Moloney murine leukemia virus (MMLV) drives luciferase expression in the Ba/F3-Luc/Wt cells. A single cell clone isolated by limiting dilution was used in all experiments. The subclone used in this study was different from that used in the previous study [3] and was selected because of its consistent in vivo proliferation. The p190 BCR-ABL gene is important in the development of acute lymphoblastic leukemia [26] and causes factor-independent, autonomous proliferation when transformed into Ba/F3 cells [27]. The Ba/F3-Luc/Wt cells were maintained in RPMI-1640 medium (Invitrogen, Grand Island, NY, USA) supplemented with 10% (v/v) fetal bovine serum (JRH Biosciences, Lenexa, KS, USA) and 1% penicillin/streptomycin (Invitrogen) in the absence of interleukin-3. Cell cultures were incubated at 37°C in 5% CO_2.

Animals

Eight-week-old female BALB/c nu/nu mice were inoculated with 2×10^6 Ba/F3-Luc/Wt cells, suspended in 0.1 mL phosphate-buffered saline (PBS), intravenously via the tail vein and were used as a hematological malignancy animal model. Mice were obtained from SLC Japan (Hamamatsu, Japan) and were handled in accordance with guidelines of the Institute of Medical Science, the University of Tokyo. Experiments were approved by the committee for animal research at the institution.

In vitro analysis

Viable cell counting, standard luciferase assay, intact-cell luciferase assay, and cell cycle analysis were performed to assess proliferation and bioluminescent features of the cultured cells. All measurements were performed in triplicate. Viable cell numbers and viability were measured using the trypan blue dye exclusion method and hemocytometers.

Luciferase activity in a given volume of cell suspension, containing various numbers of cells, was determined by a standard luciferase assay. After centrifugation of 100 μL cell suspension, the pellet was lysed with 200 μL lysis buffer (Passive Lysis Buffer; Promega). The lysate was centrifuged, and the supernatant was stored at –80°C until assayed. Luciferase activity in the supernatant was measured using the Luciferase Assay Reagent (Promega), according to the manufacturer's recommendation and using a plate reader (Wallac ARVO MX 1420 Multilabel Counter; Perkin Elmer Japan, Yokohama, Japan). Luminescence was also measured by simply adding D-luciferin (Beetle Luciferin Potassium Salt; Promega) to the cell suspension without cell lysis. We refer to this as the intact-cell luciferase assay. Cell suspension (20 μL) was added to D-luciferin (100 μL 180 μg/mL solution), and the light output was measured using the plate reader. Phenol red-free RPMI-1640 medium was used for the cell culture study to avoid possible light absorbance by the dye.

To assess the cell cycle, cells were fixed with cooled 70% ethanol. Afterward, fixed cells were washed twice with PBS and incubated with 0.5% ribonuclease A for 30 minutes. After the addition of propidium iodide (final concentration, 25 μg/mL), cells were analyzed by flow cytometry using a FACSCalibur flow cytometer (Becton Dickinson, Franklin Lakes, NJ, USA). The cell cycle was determined using the FlowJo software (TreeStar, San Carlos, CA, USA). The fraction of proliferating cells, or the proliferation index, was calculated by the following equation:

$$\text{Proliferation index}(\%) = (G_2/M+)/(G_1/G_0 + SG_2/M + S) \times 100,$$

where G_2/M, S, and G_1/G_0 are the numbers of cells in the G_2/M, S, and G_1/G_0 phases, respectively.